Bonding Analysis in Inorganic Transition-Metal Cubic Clusters, 4[+] The Distorted $Pd_9(\mu:\eta^5,\eta^2\text{-}As_2)_4(PPh_3)_8$ Architecture

Régis Gautier,[a] Jean-François Halet,*[a] and Jean-Yves Saillard*[a]

Keywords: Electron counting / Electronic structure / Density functional calculations / Extended Hückel calculations / Cluster compounds / Cluster compounds

Extended Hückel and density functional calculations were carried out on the title compound **1**. Results indicate that the bonding of the interstitial Pd_i atom with the D_{2d} distorted $(Pd_s)_8(As_2)_4$ cubic host differs from that found in the related metal-centered cubic species $M_9(\mu_4\text{-}E)_6L_8$. Species **1** can be described as an approximate square-planar 16-electron Pd_iL_4 center bound through Pd_i–As rather than Pd_i–Pd_s contacts to a distorted cubic fragment composed of four 30-electron bimetallic Pd_2L_8 units. Although a substantial gap is computed between the highest occupied molecular orbital and the lowest unoccupied molecular orbital for the observed electron count of 130 MVEs, calculations indicate that such an architecture should be observed for different electron counts close to that count. The incorporation of the central Pd atom does not seem to be essential to ensure the stability of the distorded $Pd_8(As_2)_4(PH_3)_8$ cluster. Such empty clusters, with formally four M–M bonds and eight planar 16-electron Pd_s centers, should exist for electron counts close to 120 MVEs.

Introduction

Because of potential applications in nanoelectronics, the miniaturization of solids to cluster size is an area of active research.[1] Initially restricted to metals, this field has rapidly been extended to ligated metal clusters. Among the latter, systems where a metal cube is bridged by different heavy main group atoms constitute now an important and fascinating family, which can be regarded as nanoscaled cutouts of bulk transition metal pnictides and chalcogenides. These cubic arrays may be empty or centered by an interstitial atom.[2−18] Theoretical calculations performed on empty $M_8(\mu_4\text{-}E)_6L_8$ clusters[19] and metal-centered $M_9(\mu_4\text{-}E)_6L_8$[20] (M = transition metal, E = group 14, 15, and 16 element, L = two-electron donor ligand) have shown that such compounds are characterized by an electronic structure which is either "molecular" (closed-shell electron configuration) or "metallic" (open-shell electron configuration) in nature, depending upon the electron count and the nature of the capping ligands.[21]

When omnicapped, such clusters depict generally a rather regular cubic arrangement. Expanding or shrinking of the cube is observed upon variation of the number of metal valence electrons (MVE), which ranges from 99 to 120 MVEs for empty $M_8(\mu_4\text{-}E)_6L_8$ species and from 121 to 130 MVEs for metal-centered $M_9(\mu_4\text{-}E)_6L_8$ clusters so far.[19−21] On the other hand, distorted cubic architectures are encountered when the ligand environment of the metallic cage is nonsymmetrical. This is observed for instance in the 127-MVE species $[Co_9(\mu_5\text{-}Bi)_4(CO)_{16}]^{2-}$, characterized by Eveland and Whitmire.[22] Being viewed as a metal-centered elongated Co_8 cube with four Bi atoms capping the four rectangular faces, such a cluster bears some structural resemblance to the hexacapped cubic $M_9(\mu_4\text{-}E)_6L_8$ compounds. A theoretical analysis of the bonding in this tetracapped compound and in related compounds has been recently published.[21,23]

An alternative distortion of a metal-centered M_9 cube is encountered in the related cluster $Pd_9(\mu:\eta^5,\eta^2\text{-}As_2)_4(PPh_3)_8$ (**1**), characterized by Fenske and Persau some years ago.[14] In this compound, the nine Pd atoms build up an approximate body-centered cube of D_{2d} symmetry, with four short [average Pd(1,2)−Pd(4,3) = 2.88 Å], four long [average Pd(3)−Pd(4) = 3.16 Å], and four very long [average Pd(1)−Pd(2) = 4.45 Å] distances between surface Pd (Pd_s) centers. This D_{2d} distortion of an M_8 cube is sketched in

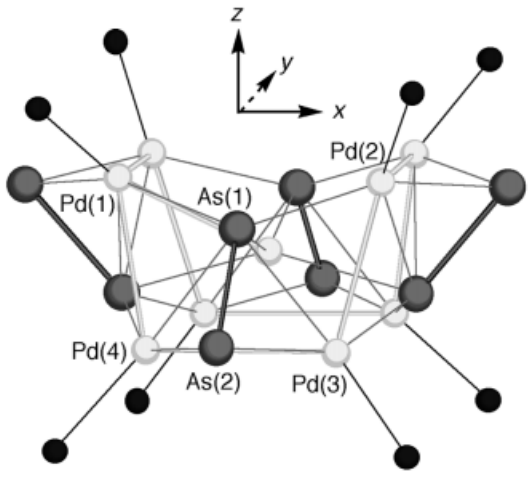

1

[+] Part 3: Ref.[23]

[a] Laboratoire de Chimie du Solide et Inorganique Moléculaire, UMR CNRS 6511,
Université de Rennes 1, 35042 Rennes Cedex, France
Fax: Int. code + 2 99 38 34 87
E-mail: halet@univ-rennes1.fr

  1434−1948/99/0404−0673 $ 17.50+.50/0

Figure 1. Rather long separations, ca. 3.00−3.09 Å are also observed between Pd_s atoms and the interstitial Pd (Pd_i) atom. Four faces of this highly distorted cube are asymmetrically capped by (μ:η^5,η^2-As_2) dumb-bells. The central Pd_i atom is bound to four As atoms (Pd_i−As = 2.57 Å) in an approximate square-planar arrangement, somewhat distorted toward tetrahedral. The As−As separation is rather short (2.36 Å) suggesting some π-bonding. The atoms constituting each As_2 units have a different environment. The As(1) atoms are connected to five metal atoms, one of them being Pd_i. Among the four As(1)−Pd_s bonds, two of them are shorter [average Pd(1,2)−As(1) = 2.49 Å] while the remaining two are quite long [average Pd(3,4)−As(1) = 2.61 Å]. The pyramidally tricoordinated As(2) atom is bonded to two Pd_s atoms [average Pd(3,4)−As(2) = 2.44 Å].

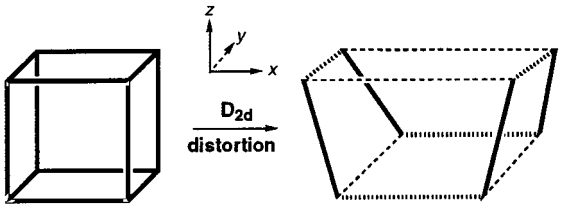

Figure 1. Conceptual formation of the D_{2d} distorted cubic $Pd_8(PH_3)_8$ fragment present in model **1**-H. Dashed lines and dotted lines correspond to long (ca. 3.15 Å) and very long (ca. 4.45 Å) metal−metal contacts, respectively.

Leaving a non-bonding lone pair on As(2), one can count the neutral (μ:η^5,η^2-As_2) units as six-electron donor ligands, which leads to a total of 130 MVEs for **1**. This renders this cluster isoelectronic to the regular cubic $Pd_9(\mu_4\text{-Te})_6(PEt_3)_8$ species.[16] Extended Hückel Theory (EHT) and Density Functional Theory (DFT) calculations were undertaken on the model compound $Pd_9(\mu:\eta^5,\eta^2\text{-}As_2)_4(PH_3)_8$ (**1**-H) to understand the unusual bonding situation in this compound (see the Appendix for the computational details). We discuss the results in this paper.

The Empty Distorted $Pd_8(As_2)_4(PH_3)_8$ Cube

The electronic structure of compound **1**-H can be formally analyzed as resulting from the interaction between the interstitial Pd_i atom and its $Pd_8(As_2)_4(PH_3)_8$ host. On the other hand, the molecular orbital (MO) diagram of the D_{2d} $Pd_8(As_2)_4(PH_3)_8$ fragment itself can be derived from the interaction of the four noninteracting $[As_2]^{4-}$ units (As−As single bonds are assumed) with the distorded $[Pd_8(PH_3)_8]^{16+}$ fragment. The frontier molecular orbitals (FMO) of the latter itself descend from those of a regular cubic cage. Indeed, starting with a regular cube, the metal framework found for **1** can be generated according to a D_{2d} distortion by elongating parallel metal−metal edges of the top and bottom faces of the cube as illustrated in Figure 1. Therefore, it is important to evaluate first the effects of the D_{2d} distortion on the skeletal MOs of an idealized $Pd_8(PH_3)_8$ cube. The qualitative analysis developped below is based on EHT calculations (see Appendix for details).

The MO diagram of the idealized $Pd_8(PH_3)_8$ cube of O_h symmetry (Pd−Pd = 2.88 Å) can be qualitatively obtained by combining the FMOs of the eight $Pd(PH_3)$ units.[19a,21] Such a fragment, as shown on the far left-hand side of Figure 2, presents a block of five d-type orbitals (one, two, and two of σ, π, and δ symmetry, respectively) below a radial σ-type sp hybrid and a set of two tangential π-type orbitals of Pd 5p parentage.[19a] When the cube is built, the three upper diffuse FMOs (sp_σ and p_π) of the eight $Pd(PH_3)$ groups overlap strongly and generate a set of 12 bonding MOs, largely separated from a set of 12 antibonding MOs. The more contracted d-type FMOs give rise to a band of 40 combinations which spreads out over a range of about 1 eV. Unlike for the s and p orbitals, the d-type overlap is not strong enough to create an energy gap separating the in-phase combinations from the out-of-phase ones. In our chosen fragment charge partitioning, the eight upper orbitals of the d-band are formally vacant. The derivation of the MO level ordering of the regular $[Pd_8(PH_3)_8]^{16+}$ cube from the $Pd(PH_3)$ FMOs is sketched in Figure 2a.

Upon D_{2d} distortion which leads to four long and four very long metal−metal separations (see Figure 1), the MO diagram of $[Pd_8(PH_3)_8]^{16+}$ is perturbed as shown in Figure 2b. Because of the lengthening of eight edges of the cube, some antibonding and bonding metal−metal MOs become nonbonding. EHT calculations indicate that the overlap between the s and p Pd FMO's is cancelled along the four 4.45 Å very long edges while it is still significant along the four 3.16 Å long Pd−Pd edges. As a result, four s and p-type antibonding combinations are significantly stabilized, leading to a set of eight antibonding orbitals and a set of 16 bonding/nonbonding orbitals. The overlap between the more contracted d-type orbitals remains significant only on the four 2.88 Å short edges. Whithin the d-band, this leads to the concentration of most of the Pd−Pd bonding character over a set of four orbitals of a_1, b_1, and e symmetry. These four orbitals lie at the very bottom of the band. They are preponderantly localized on the short edges of the distorted cube and have the proper symmetry to be considered as holding four localized Pd−Pd bonding pairs.

With formally a single bond between the As atoms, the seven occupied MOs of an isolated $(As_2)^{4-}$ unit separate into one low-lying σ-bonding orbital and six more or less nonbonding MOs which can be associated with the six lone pairs of the saturated $(As_2)^{4-}$ species. Four of these six orbitals are the in-phase (weakly bonding) and out-of-phase (weakly antibonding) combinations of the 4p(π) As orbitals, the remaining 2 being of σ-type. Because of the large energy separation between the 4s and 4p shells in As, one of the σ-nonbonding combinations, being largely 4s in character, lies at very low energy. Considering that the empty antibonding σ* level is situated at a very high energy, one is left for each $(As_2)^{4-}$ unit with 5 MOs (4 of π-type, 1 of σ-type) lying at a moderate energy and consequently susceptible to significantly interact with the $[Pd_8(PH_3)_8]^{16+}$ cube. These orbitals, all occupied, are sketched on the far right-hand side of Figure 2. When brought together, the frontier orbitals of the $(As_2)^{4-}$ groups give rise to a set of

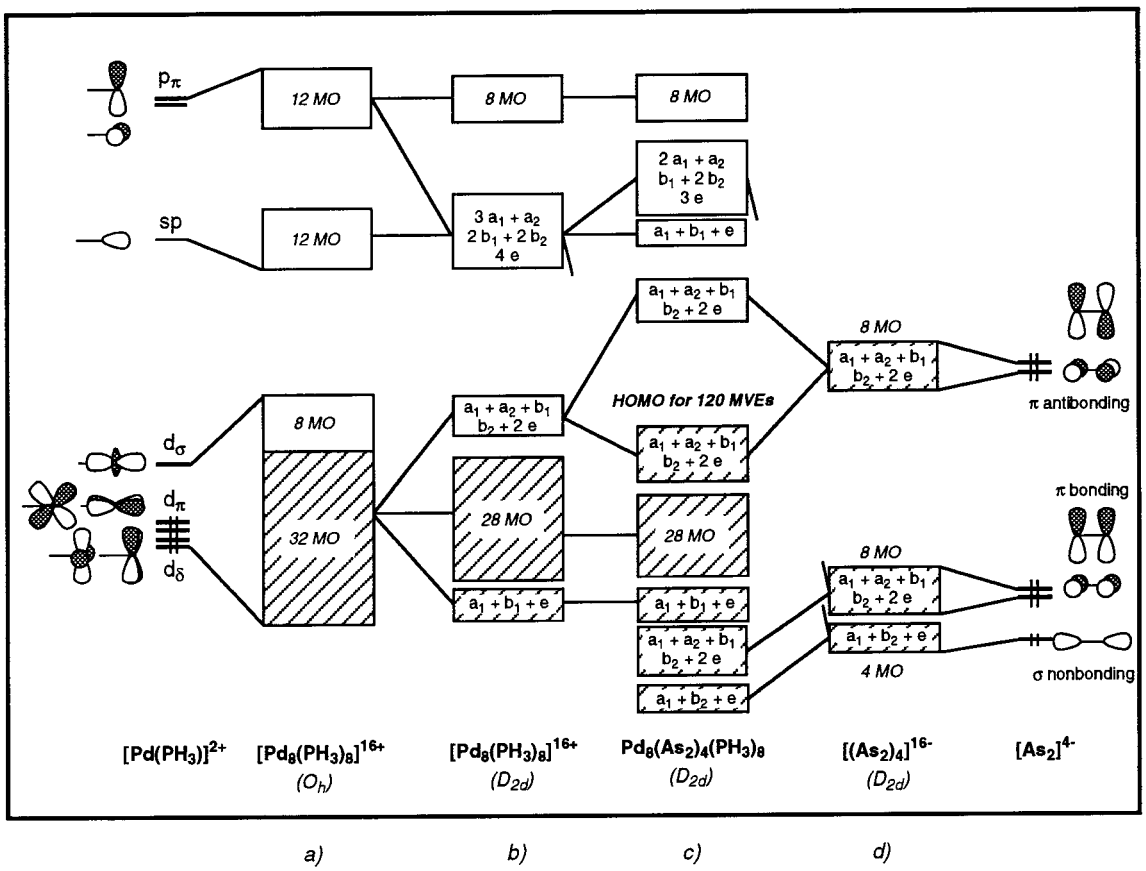

Figure 2. Qualitative MO diagrams based on EHT calculations for the idealized (12 M−M bonds) (a) and distorted (4 M−M bonds) (b) $[Pd_8(PH_3)_8]^{16+}$ fragment, the empty distorted $Pd_8(PH_3)_8(As_2)_4$ cluster (c), and the $[(As_2)_4]^{16-}$ fragment (d). The FMOs of the $Pd(PH_3)$ and As_2 moieties are shown on the far left- and far right-hand sides, respectively.

four combinations of the σ FMOs, lying close to a set of 8 combinations of the π FMOs, separated from the 8 π* combinations, as shown in Figure 2d.

The MO diagram showing the major bonding interactions between the two $[(As_2)_4]^{16-}$ and $[Pd_8(PH_3)_8]^{16+}$ fragments is given in Figure 2c. The twenty occupied FMOs of the former need to find vacant metallic counterparts of the same symmetry in the latter. These twenty metallic FMO's originate from two groups. One of them is made of the 8 d-type vacant orbitals, of symmetry $a_1 + a_2 + b_1 + b_2 + 2\times$ e. The second group, of symmetry $2\times a_1 + a_2 + b_1 + 2\times b_2 + 3\times$ e, is made of 12 among the sixteen s- and p-type bonding/nonbonding combinations. The interaction between the two fragments leads to the formation of twenty bonding and twenty antibonding combinations, as illustrated in Figure 2. Applying the closed-shell requirement to the hypothetical $Pd_8(PH_3)_8(As_2)_4$ model leads to the favored 120-MVE count. For this peculiar electron count, EHT calculations give a gap of 0.90 eV between the highest occupied molecular orbital (HOMO) and the lowest unoccupied molecular orbital (LUMO). The computed overlap population corresponding to the short Pd−Pd distances is rather weak [Pd(1,2)−Pd(3,4) = 0.03], whereas those corresponding to the long and very long Pd−Pd separations are nearly equal to zero. The significant participation to vacant levels of the π* FMOs of the $(As_2)^{4-}$ units provide the As−As single bonds with some additional π-bonding character, as shown by the increase of the As-As overlap population relative to an isolated $(As_2)^{4-}$ unit [0.92 in $Pd_8(PH_3)_8(As_2)_4$ vs 0.53 for the free $(As_2)^{4-}$ group]. The Pd−As overlap populations [Pd(1,2)−As(1) = 0.30, Pd(3,4)−As(1) = 0.18, and Pd(3,4)−As(2) = 0.38] suggest that the As atoms are firmly bonded to the eight Pd atoms.

To gain some confidence in the EHT results, DFT calculations were undertaken on the 120-MVE $Pd_8(PH_3)_8(As_2)_4$ model. Full optimization was made under the D_{2d} symmetry constraint. The optimized bond lengths for this model are given in Table 1 along with those obtained for the 130-MVE metal-centered $Pd_9(\mu{:}\eta^5,\eta^2\text{-}As_2)_4(PH_3)_8$ species. Remarkably, the computed distances are similar overall in the empty and the metal-centered clusters. We shall come back to this point in the next section. A HOMO-LUMO gap of 0.73 eV (comparable to that obtained from EHT calculations) is computed. These results suggest that empty clusters such as $Pd_8(As_2)_4(PH_3)_8$ with a D_{2d} distorted cubic framework may exist.

The fact that each $(As_2)^{4-}$ ligand uses only five FMOs for making six Pd−As "bonds" is typical of hypervalency.[24] However, as for the diamagnetic 120-MVE $M_8(\mu_4\text{-}E)_6L_8$ clusters, it is possible to describe $Pd_8(PH_3)_8(As_2)_4$ with a

simple 2-electron/2-center localized bonding scheme in which the number of bonding electron pairs is necessarily larger than the number of bonding combinations appearing in the delocalized MO diagram.[19] Assuming four Pd−Pd bonds, 24 Pd−As bonds, and four As−As bonds, the triconnected As(2) atoms hold a lone pair and satisfy the octet rule while the hypervalent As(1) atoms are 10-electron centers. Interestingly, within this bonding scheme, the Pd atoms are 16-electron centers, a typical configuration for the planar coordination mode.[24] As a matter of fact, a careful structural analysis of **1** indicates a not-far-from planar ligand environment around the Pd_s atoms. In the $Pd_8(PH_3)_8(As_2)_4$ model, the geometry of which is taken from the idealized geometry of **1**, the two strongest Pd−As bonds and the Pd−P bond are almost in the same plane for each metal center, whereas the weaker Pd−As bond is about 10° away from this plane. From this point of view, the hypothetical 120-MVE $Pd_8(As_2)_4(PH_3)_8$ cluster can be considered as the assemblage of four 30-electron $L_4Pd-PdL_4$ units, made of two 16-electron centers and linked to each other via bridging As_2 ligands (i.e. $4 \times (2 \times 16 - 2) = 120$ MVEs). It is related to a series of 128-MVE Cu_8 clusters which can be described as resulting from the assemblage of eight 16-electron square-planar systems, with no formal metal−metal bonding (except perhaps some $d^{10}-d^{10}$bonding).[26] Adding formally 8 electrons to $Pd_8(PH_3)_8(As_2)_4$ would break the four Pd−Pd bonds, making the system isoelectronic to the Cu_8 species.

Encapsulation of the Interstitial Metal Atom

The qualitative MO diagram of the metal-centered $Pd_9(\mu:\eta^5,\eta^2\text{-}As_2)_4(PH_3)_8$ cluster (**1**-H) illustrating the major interactions between Pd_i and its metallic host is shown in Figure 3. According to EHT calculations, only four among the 9 Pd_i atomic orbitals interact with the empty cage. The 5s and 5p(*x,y*) orbitals (of symmetry a_1 and e, respectively) are strongly destabilized by occupied counterparts of the $Pd_8(PH_3)_8(As_2)_4$ cage. After interaction, the occupation of the 5s and 5p(*x,y*) orbitals is 0.33 and 0.24, respectively. The fourth Pd_i orbital which is involved in the bonding is the low-lying and occupied x^2-y^2 orbital, of b_2 symmetry, which is stabilized by the lowest unoccupied b_2 level of the cage which has a large As−As π* character. After interaction, the x^2-y^2 population is 1.72. The other d-type orbitals of Pd_i do not interact, as well as the 5p(*z*) orbital which remains almost unperturbed with an occupation close to zero (0.03). It is noteworthy that the FMOs of the host which interact with Pd_i are mainly localized on the As(1) atoms overall and rather poorly on the As(2) and Pd_s atoms. This was expected owing to the short Pd_i−As(1) distances (ca. 2.57 Å). Since Pd_i is situated in an approximately square-planar environment of As(1) atoms, it is thus not surprising that it uses its s, *x*,*y*, and x^2-y^2 orbitals for bonding. Four Pd_i−As(1) bonding pairs can be identified. Three of them, of a_1 and e symmetry, are provided by the empty cage and donated to the metal. The fourth bonding pair, of b_2 symmetry, is provided by the metal x^2-y^2 orbital and donated to the cage (mainly to the As−As π* orbitals). Therefore, Pd_i can be described as a d^{10} square-planar 16-electron center. From the point of view of total cluster electron count, it is important to note that the three electron pairs, which are donated by the cage to Pd_i, are already involved in the bonding within the cage. Since they cannot be counted twice, the total MVE count can be formulated as 120 (empty cage) + 16 (Pd_i) − 6 (delocalized bonding electrons) = 130 MVEs.

As expected from the above discussion, the Pd_s-Pd_i overlap population is very weak. On the other hand, the Pd_i−As(1) overlap populations are strong, ca. 0.22, comparable to the Pd_s−As overlap populations which are 0.27 on average. As in the empty $Pd_8(As_2)_4(PH_3)_8$ parent cluster, the overlap populations corresponding to the long and very long Pd_s-Pd_s separations are nearly zero, whereas those corresponding to the short Pd_s-Pd_s contacts are ca. 0.02. The different Pd_s−As overlap populations [Pd(1,2)−As(1) = 0.30, Pd(3,4)−As(1) = 0.16, and Pd(3,4)−As(2) = 0.36] and As−As OP (0.91) are comparable to those computed for the empty parent cluster (vide supra). DFT calculations were carried out on **1**-H in order to support the EHT orbital analysis. The Pd_s-Pd_s and Pd_s−As separations obtained from a full optimization of **1**-H under the D_{2d} symmetry constraint indicate, as suggested from the EHT calculations, that the insertion of the central Pd atom hardly modifies the geometry of the distorted $Pd_8(As_2)_4(PH_3)_8$ cube. The geometries are highly similar

Table 1. Comparison of the calculated and experimental distances [Å] for empty and metal-centered distorted cubic models

Compound	$Pd_8(As_2)_4(PH_3)_8$[a]	$Pd_9(\mu:\eta^5,\eta^2\text{-}As_2)_4(PH_3)_8$[a]	$Pd_9(\mu:\eta^5,\eta^2\text{-}As_2)_4(PPh_3)_8$[b]
Pd_i-Pd_s	−	3.06	3.04
Pd(1-2)−Pd(4-3)	2.98	2.97	2.88
Pd(3)−Pd(4)	3.14	3.06	3.16
Pd(1)−Pd(2)	4.27	4.52	4.46
Pd_i−As(1)	−	2.60	2.57
Pd(1-2)−As(1)	2.49	2.52	2.44
Pd(1-2)−As(2)	2.52	2.53	2.49
Pd(3-4)−As(2)	2.56	2.67	2.61
As(1)−As(2)	2.30	2.31	2.36

[a] Calculated structure. − [b] Experimental structure.

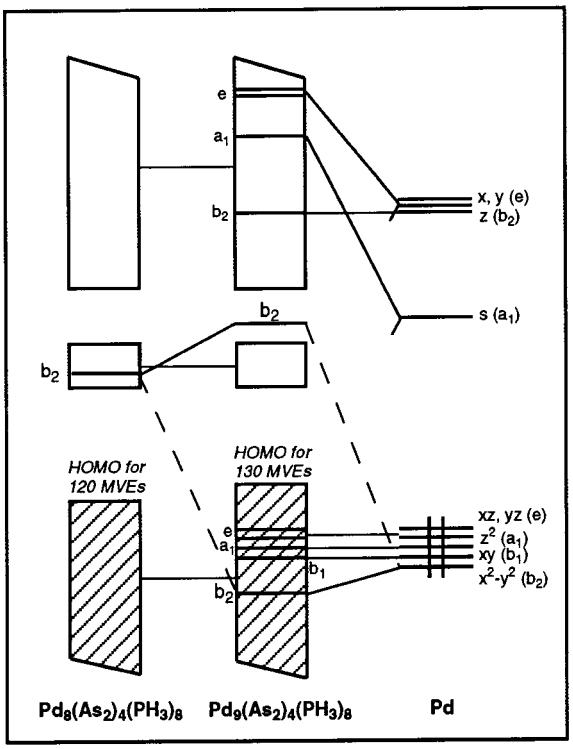

Figure 3. Qualitative MO diagram based on EHT calculations for the metal-centered species **1**-H obtained from the interaction of the distorted cubic $Pd_8(As_2)_4(PH_3)_8$ fragment with the interstitial Pd atom

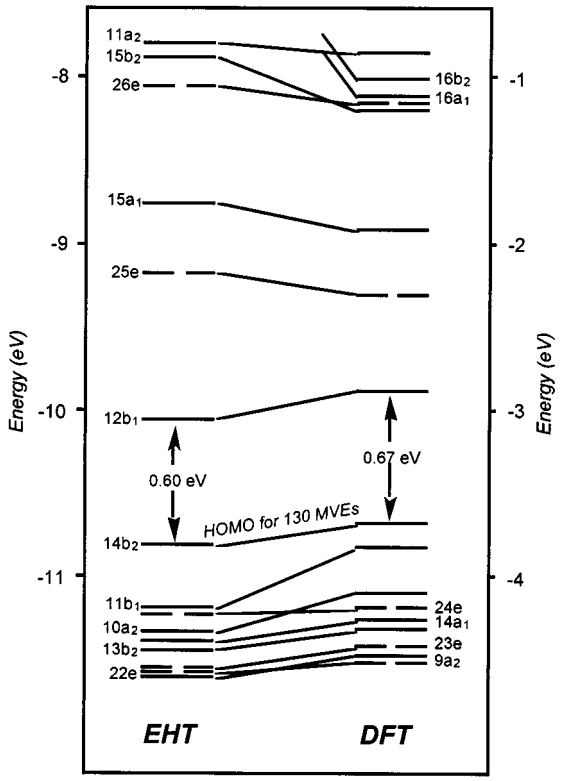

Figure 4. EHT (left) and DFT (right) MO diagrams for **1**-H

(see Table 1). The potential energy surface is particularly flat around the energy minimum, indicating that such an arrangement is rather flexible. A rather good agreement is observed between the optimized geometry of **1**-H and the experimental geometry of **1**. The largest deviation concerns the short Pd_s-Pd_s distance, computed to be 0.09 Å longer than the experimental value. This provides compelling evidence that the DFT approach is reliable for predicting the bond lengths of large inorganic transition metal systems.

The DFT and EHT MO diagrams of **1**-H are compared in Figure 4. They are similar overall, exhibiting the same ground-state electronic configuration. Both calculations predict a closed-shell configuration for the count of 130 MVEs. Note that a single-point DFT calculation on compound **1**, that is in which the PH_3 ligands were replaced by PPh_3 ligands, lead to similar results.

According to Figure 4, several empty MOs lie in the middle of a large energy gap separating the HOMO $14b_2$ from the high-lying 26e MO. One may ask whether reduced species would be stable. EHT calculations indicate that populating the $12b_1$ LUMO hardly changes the nature of the bonding in the cluster. Mono- or di-anionic species should be possible. Conversely, oxidation of compound **1** may be possible since the $14b_2$ HOMO is somewhat Pd_s-Pd_i antibonding. Its complete or partial depopulation should lead to some shrinking of $Pd_8(As_2)_4$ and enhance the Pd_s-Pd_i bonding. In other words, in comparison with other cubic M_8 and M_9 architectures which are observed for a large range of electron counts,[19–21,23] arrangements such as **1** should be observed for different electron counts with either closed- or open-shell electron configurations.

Conclusion

The theoretical analysis of $Pd_9(\mu{:}\eta^5,\eta^2\text{-}As_2)_4(PPh_3)_8$ shows that the bonding of the interstitial Pd atom with the D_{2d} distorded $Pd_8(As_2)_4$ cubic host differs from that found in its related metal-centered cubic species $M_9(\mu_4\text{-}E)_6L_8$ in which the bonding was ensured by strong bonding interactions between the central and surface metal atoms. Indeed, in compound **1** the central atom can be described as a roughly square-planar 16-electron center, bound through Pd_i-As rather than Pd_i-Pd_s contacts to a distorted cubic fragment made of four 30-electron bimetallic Pd_2L_8 units, each Pd_2L_8 unit being made of two approximately planar PdL_4 16-electron centers linked by a Pd–Pd bond. Since six metal-ligand bonding electrons are shared by the cage and the Pd_i center, the cluster electron count can be decomposed as follow: $8 \times (2 \times 16 - 2) + 16 - 6 = 130$ MVEs. A strongly different bonding picture was computed for the isoelectronic 130-MVE $Ni_9Te_6(PEt_3)_8$ species.[20] A substantial HOMO–LUMO gap is computed for the observed electron count of 130 MVEs, a situation generally encountered in stable molecular compounds. However, our calculations indicate that such an architecture should be observed for a range of allowed electron counts around 130 MVEs, a common situation encountered in extended structures.

Appendix

a) Extended Hückel Calculations: Calculations have been carried out within the extended Hückel formalism[26] using the weighted H_{ij} formula[27] with the program CACAO.[28] The exponents (ζ) and the valence shell ionization potentials (H_{ii} in eV) were (respectively): 1.3, −13.6 for H 1s; 1.6, −18.6 for P 3s; 1.6, −14.0 for P 3p; 2.23, −16.22 for As 4s; 1.89, −12.16 for As 4p; 2.19, −7.32 for Pd 5s; 2.152, −3.75 for Pd 5p. H_{ii} value for Pd 4d was set equal to −12.02. A linear combination of two Slater-type orbitals of exponents $\zeta_1 = 5.983$ and $z_2 = 2.613$ with the weighting coefficients $c_1 = 0.5264$ and $c_2 = 0.6373$ was used to represent the Pd 4d atomic orbitals. The different molecular models used were based on the averaged idealized (D_{2d}) experimental structure of **1**. The following bond distances [Å] were used in the $Pd_8(As_2)_4(PH_3)_8$ and $Pd_9(As_2)_4(PH_3)_8$ models: Pd_i-Pd_s = 3.05, Pd(1,2)−Pd(4,3) = 2.88 Å, Pd(3)−Pd(4) = 3.16 Å, Pd(1)−Pd(2) = 4.45 Å, Pd_i−As(1) = 2.57 Å, Pd(1,2)−As(1) = 2.51 Å, Pd(1,2)−As(2) = 2.61 Å, Pd(3,4)−As(2) = 2.43 Å, and Pd−P = 2.26 Å.

b) Density Functional Calculations: Density Functional calculations[29] were carried out on the empty $Pd_8(As_2)_4(PH_3)_8$ and metal-centered $Pd_9(As_2)_4(PH_3)_8$ models using the Amsterdam Density Functional (ADF) program.[30] Electron correlation was treated within the local density approximation (LDA).[31] The numerical integration procedure applied for the calculations was developed by te Velde et al.[29c] The atom electronic configurations were described by a triple-ζ Slater-type orbital (STO) basis set for H 1s, P 2s and 2p, As 3s and 3p, Pd 5s and 4d, and single-z STO function for H 2p, P 3d, As 4d, and Pd 5p. A frozen-core approximation[32] was used to treat the core electrons of P, As, and Pd.

Acknowledgments

The authors thank the Centre de Ressources Informatiques (CRI) of Rennes and the Institut de Développement et de Ressources en Informatique Scientifique (IDRIS-CNRS) of Orsay for computing facilities. Prof. D. Fenske (Karlsruhe, Germany) is thanked for helpful discussions.

[1] *Clusters and Colloids, From Theory to Applications* (Ed.: G. Schmid), VCH, Weinheim, **1994**.
[2] L. D. Lower, L. F. Dahl, *J. Am. Chem. Soc.* **1976**, *98*, 5046.
[3] D. Fenske, R. Basoglu, J. Hachgenei, F. Rogel, *Angew. Chem., Int. Ed. Engl.* **1984**, *23*, 160.
[4] D. Fenske, J. Magull, *Z. Naturforsch.* **1990**, *45b*, 121.
[5] D. Fenske, H. Krautscheid, M. Müller, *Angew. Chem., Int. Ed. Engl.* **1992**, *31*, 321.
[6] D. Fenske, J. Hachgenei, J. Ohmer, *Angew. Chem., Int. Ed. Engl.* **1985**, *24*, 706.
[7] D. Fenske, J. Ohmer, J. Hachgenei, K. Merzweiler, *Angew. Chem., Int. Ed. Eng.* **1988**, *27*, 1277.
[8] D. Fenske, J. Hachgenei, F. Rogel, *Angew. Chem., Int. Ed. Engl.* **1984**, *23*, 982.
[9] G. Christou, K. S. Hagen, J. K. Bashkin, R. H. Holm, *Inorg. Chem.* **1985**, *24*, 1010.
[10] [10a] S. Pohl, U. Opitz, *Angew. Chem., Int. Ed. Engl.* **1993**, *32*, 863. – [10b] S. Pohl, W. Barklage, W. Saak, U. Opitz, *J. Chem. Soc., Chem. Commun.* **1993**, 1251.
[11] C. Junghans, W. Saak, S. Pohl, *J. Chem. Soc., Chem. Commun.* **1994**, 2327.
[12] S. Pohl, W. Saak, *Angew. Chem., Int. Ed. Eng.* **1984**, *23*, 907.
[13] J. P. Zebrowski, R. K. Hayashi, A. Bjarnason, L. F. Dahl, *J. Am. Chem. Soc.* **1992**, *114*, 3121.
[14] D. Fenske, C. Persau, *Z. Anorg. Allg. Chem.* **1991**, *593*, 61.
[15] D. Fenske, J. Ohmer, K. Merzweiler, *Angew. Chem., Int. Ed. Engl.* **1988**, *27*, 1512.
[16] J. G. Brennan, T. Siegrist, S. M. Stuczynski, M. L. Steigerwald, *J. Am. Chem. Soc.* **1989**, *111*, 9240.
[17] D. Fenske, H. Fleischer, C. Persau, *Angew. Chem., Int. Ed. Engl.* **1989**, *28*, 1665.
[18] [18a] D. Fenske, K. Vogt, unpublished results. – [18b] K. Vogt, Ph.D. Dissertation, Univ. of Karlsruhe, Germany, **1994**.
[19] [19a] E. Furet, A. Le Beuze, J.-F. Halet, J.-Y. Saillard, *J. Am. Chem. Soc.* **1994**, *116*, 274. – [19b] N. Rösch, L. Ackerman, G. Pacchioni, *Inorg. Chem.* **1993**, *32*, 2963.
[20] E. Furet, A. Le Beuze, J.-F. Halet, J.-Y. Saillard, *J. Am. Chem. Soc.* **1995**, *117*, 4936.
[21] [21a] J.-F. Halet, J.-Y. Saillard, *Struct. Bond.* **1997**, *87*, 81. – [21b] R. Gautier, J.-F. Halet, J.-Y. Saillard, in *Metal Clusters in Chemistry* (Eds. : P. Braunstein, L. Oro, P. R. Raithby), VCH, Weinheim, **1998**, in press.
[22] K. H. Whitmire, J. R. Eveland, *J. Chem. Soc., Chem. Commun*. **1994**, 1335.
[23] B. Zouchoune, F. Ogliaro, J.-F. Halet, J.-Y. Saillard, J. R. Eveland, K. H. Whitmire, *Inorg. Chem.* **1998**, *37*, 865.
[24] *Orbital Interactions in Chemistry,* T. A. Albright, J. K. Burdett, M-H Whangbo, J. Wiley & Sons, New York, **1984.**
[25] [25a] L. E. Mc Candlish, E. C. Bissell, D. Coucouvanis, J. P. Fackler, K. Knox, *J. Am. Chem. Soc.* **1968**, *90*, 7357. – [25b] F. J. Hollander, D. Coucouvanis, *J. Am. Chem. Soc.* **1974**, *96*, 5646. – [25c] F. J. Hollander, M. L. Cafferty, D. Coucouvanis, 167th National Meeting of the American Chemical Society, Los Angeles, **1974**. – [25d] A. Avdeef, J. P. Fackler, *Inorg. Chem.* **1978**, *17*, 2182.
[26] R. Hoffmann, *J. Chem. Phys.* **1963**, *39*, 1397.
[27] J. H. Ammeter, H.-B. Bürgi, J. C. Thibeault, R. Hoffmann, *J. Am. Chem. Soc.* **1978**,*100*, 3686.
[28] C. Mealli, D. Proserpio, *J. Chem. Educ.* **1990**, *67*, 399.
[29] [29a] E. J. Baerends, D. E. Ellis, P. Ros, *Chem. Phys.* **1973**, *2*, 41. – [29b] E. J. Baerends, P. Ros, *Int. J. Quantum. Chem.* **1978**, *S12*, 169. – [29c] P. M. Boerrigter, G. te Velde, E. J. Baerends, *Int. J. Quantum Chem.* **1988**, *33*, 87. – [29d] G. te Velde, E. J. Baerends, *J. Comput. Phys.* **1992**, *99*, 84.
[30] E. J. Baerends et al., *Amsterdam Density Functional (ADF) program, version 2.0.1*, Vrije Universiteit, Amsterdam, Netherlands, **1996**.
[31] S. D. Vosko, L. Wilk, M. Nusair, *Can. J. Chem.* **1990**, *58*, 1200.
[32] E. J. Baerends, Ph. D. Thesis, Vrije Universiteit, Amsterdam, Netherlands, **1975**.

Received September 24, 1998
[I98325]